
INVESTIGATING THERMAL TRANSPORT IN KNOTTED GRAPHENE NANORIBBONS USING NON-EQUILIBRIUM MOLECULAR DYNAMICS

A PREPRINT

Levi C. Felix, Alexandre F. Fonseca and Douglas S. Galvao*

Department of Applied Physics
State University of Campinas
Campinas, SP 13083-970, Brazil

August 4, 2022

ABSTRACT

In this work, we investigated the effect of knots in the thermal transport of graphene nanoribbons through non-equilibrium molecular dynamics simulations. We considered the cases of one, two, and three knots are present. Temperature jumps appear in the temperature profile where the knots are located, which indicates that they introduce thermal resistances in the system, similar to interfacial Kapitza resistance present between two different materials and/or single materials with defects and/or lattice distortions. We found that the thermal resistance introduced by each individual knot is essentially the same as the overall resistance increase linearly with the number of knots, as they behave as thermal resistances associated in series. Also, the relative position between each knot in the arrangement does not strongly affect the thermal current produced by the temperature gradient, showing a weak thermal rectification effect.

Keywords Graphene nanoribbons · Thermal transport · Non-equilibrium molecular dynamics

1 Introduction

Among all graphene-derived nanostructures, graphene nanoribbons (GNRs) have received much attention from the materials physics community due to their quasi-one-dimensional character and topological simplicity, as they are only narrow and straight-edged stripes of graphene. Particularly, the electronic properties have been found to strongly depend on the edge type (armchair or zigzag) [1, 2, 3, 4] where localized states appear at the edges of zigzag GNRs but not on zigzag ones. More recently, even some topological phases under external electric fields and boron/nitrogen doping have been reported [5]. This creates perspectives for GNRs to be a competitive candidate material in quantum electronics applications [6]. For such applications, it is also important to study their thermal transport since there is always a heating-up/cooling-down cycle in electronic devices. For most low-dimensional materials, thermal transport is expected to be influenced by surface roughness where the majority of phonon scattering processes take place [7, 8]. For GNRs, however, the mean free path of the dominant phonon mode (~ 1 nm) is much larger than the mean height variation at the surface ($0.2 - 0.6$ Å) [9]. The successful experimental synthesis of GNRs [10, 11, 12] has made possible the investigation of their electronic [13] and thermal [14] transport properties, which opens many possibilities for industrial large-scale applications.

Defect engineering of GNRs is a common strategy to improve and tune some properties that otherwise are not observed in non-defective nanoribbons. Examples include spin filtering by combining vacancies and doping with boron and nitrogen atoms [15], and bandgap tuning through edge patterning by interacting with vacancy defects [16]. Geometrical distortions, such as twists and knots, have also been considered to obtain new behavior in addition to point and edge defects. The possible formation of twisted GNRs was already discussed [17, 18], where a helix configuration was

*Corresponding author: galvao@ifi.unicamp.br

found to be more favorable than a simple torsion. Also, the charge carrier type and mobility could also be tuned by the degree of twisting and turning on GNRs helices [19]. Other interesting findings on twisted GNRs include unique properties for different conformations of the nanoribbons [20], presence of non-linear current-voltage characteristics with an applied transverse electric field [21], structural strengthening effect when they are inside carbon nanotubes [22], and even chirality-controlled carbon nanotube synthesis [23]. Knots are also another sort of material distortion that have been investigated in carbon materials like carbon nanotubes [24], microfibers [25, 26], graphene oxides [27], silk fibers [28], and GNRs [29]. Particularly, knotted GNRs were found to possess two metastable configurations at two distinct stretching levels and a spin-polarized electronic ground state in the tight-knot case.

Extensive mechanical properties studies in knotted nanostructures have already been reported in the literature [24, 25, 26, 27, 28, 29], but very few have been focused on investigating heat transport. In this way, in the present work, we investigated the influence of knots GNRs on the heat flux generated by the presence of two thermal contacts at distinct temperatures that creates a temperature gradient. For this purpose, we considered the presence of one, two, and three knots. For direct comparison, we have also considered the cases of the structures without defects nor twists, to better evaluate the role played by such distortions on the thermal transport of knotted GNRs.

2 Methods

To build a knotted hydrogen passivated GNR, we created a straight structure with width of $W = 10 \text{ \AA}$ using the Visual Molecular Dynamics (VMD) software. Then, with the help of the sculptor tool, we considered a set of four points where the nanoribbon is mapped to obtain a pre-knotted structure that is shown in the snapshot 1 of the Figure 1. Then, using fully atomistic reactive molecular dynamics simulations, we stretched the whole structure until the knot is closed, as shown in the snapshots 2-4 of Figure 1. We repeated the same process to create the two and three-knot GNRs shown in Figure 1 at the bottom. The distance between each knot was chosen to be $d = 60 \text{ \AA}$ and the total length $L = 3 \text{ nm}$. As mentioned above, for comparison we also considered a GNR without knots with the same length.

We considered all nanoribbons in this work to be suspended by fixing both of their ends, as illustrated by Figure 2. We investigated the thermal transport of knotted GNRs through molecular dynamics (MD) simulations using the LAMMPS code [30]. We first equilibrated all GNRs using an NVT ensemble during 100 ps to determine their structural and thermal stability. The interaction among all carbon atoms is described by the Tersoff potential, with the optimized set of parameters obtained by Lindsay and Broido [31] to better describe the thermal properties of graphene. Then, we set two Nosé-Hoover thermostatted regions with a 40 \AA -length near both fixed ends as can be seen in Figure 2. These regions play the role of thermal baths at $T_{\text{hot}} = 500 \text{ K}$ and $T_{\text{cold}} = 300 \text{ K}$ to induce a temperature gradient in the GNRs and, consequently, a heat current that flows from the hot to the cold reservoir. The process of building a temperature gradient is performed by running an NVT MD only for the thermostatted regions and an NVE dynamics for the atoms between the two thermal reservoirs during 1 ns. This ensures that the system reaches a steady state where the energy that enters the cold reservoir is equal in magnitude but opposite in signal to the energy that goes out from the hot one. A similar methodology has been proved to agree well with experimentally-obtained results for pristine graphene [32, 33].

In Figure 2 we present an example of the spatial temperature distribution for a three-knot nanoribbon. Following the equipartition theorem, a 'temperature' per atom is defined as $t = k_{\text{at}}/k_{\text{B}}/1.5$ with k_{at} the kinetic energy per atom, and k_{B} the Boltzmann constant. This is defined in a way that the sum of t over all atoms yields the temperature of the system. The temperature value of each atom in Figure 2 is given by the spatial average of all t values of atoms within a cutoff radius of 5 \AA as performed by OVITO [34]. After setting the thermal gradient, we carried out an MD run for another 1 ns to calculate the temperature profile and monitor the cumulative energy that goes in (out) to (from) the cold (hot) reservoir.

The heat current J is defined as the slope of the cumulative energy as a function of time. Using the one-dimensional Fourier's law of heat conduction, the heat flux q can be estimated by

$$q = \frac{J}{A} = \kappa \frac{dT}{dx}, \quad (1)$$

where A is the cross-sectional area given by $W * 3.35 \text{ \AA}$, with 3.35 \AA being the thickness of a graphene monolayer, dT/dx the temperature gradient, and κ the thermal conductivity of the system.

Discontinuities in the temperature profile of ΔT characterize a thermal resistance. This concept is usually used when there is an interface between two different materials, which defines the so-called interfacial thermal resistance, or the Kapitza resistance [35] that is given by

$$R = \frac{\Delta T}{q}. \quad (2)$$

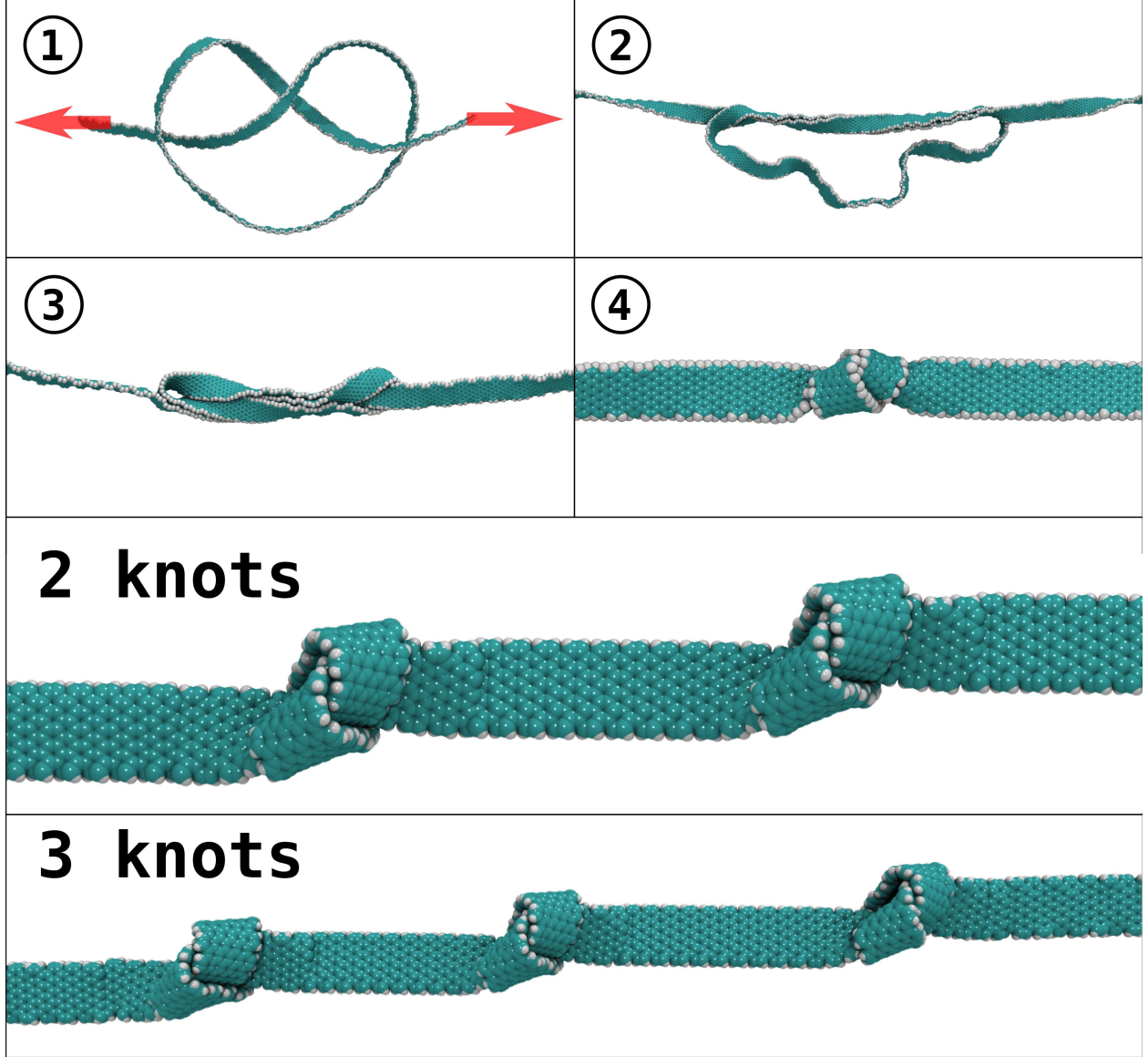


Figure 1: Sequential snapshots showing the process of tying the knot in hydrogen passivated GNR (1-4). Two and three-knot structures are shown at the bottom, where each knot is 60 Å apart. Green and white colors indicate carbon and hydrogen atoms, respectively.

Although R is defined for situations when there are two different materials, where this resistance is a result of a heat current flowing through two media with different thermal conductivity, the Kapitza resistance was already reported to exist in structures made out of a single material but with the presence of defects [36, 37, 38, 39] and lattice distortions [40, 41, 42, 43, 44].

3 Results

The temperature profile of GNRs without, with one, two, and three knots are presented in Figure 3. The red lines highlight the flat regions in the nanoribbon, where the temperature gradient is approximately linear and have a constant dT/dx . The green lines correspond to dT/dx where the knots are located. For the case without knots, a well defined linear behavior can be observed in the Figure 3 (a), where the profile changes exponentially near the thermal baths due to phonon scattering at the interfaces between the regions that are thermostatted and those that are not [45, 46, 47]. From one to three-knot cases (Figures 3 (b)-(d)), a temperature jump is observed at each knot, where the the slope

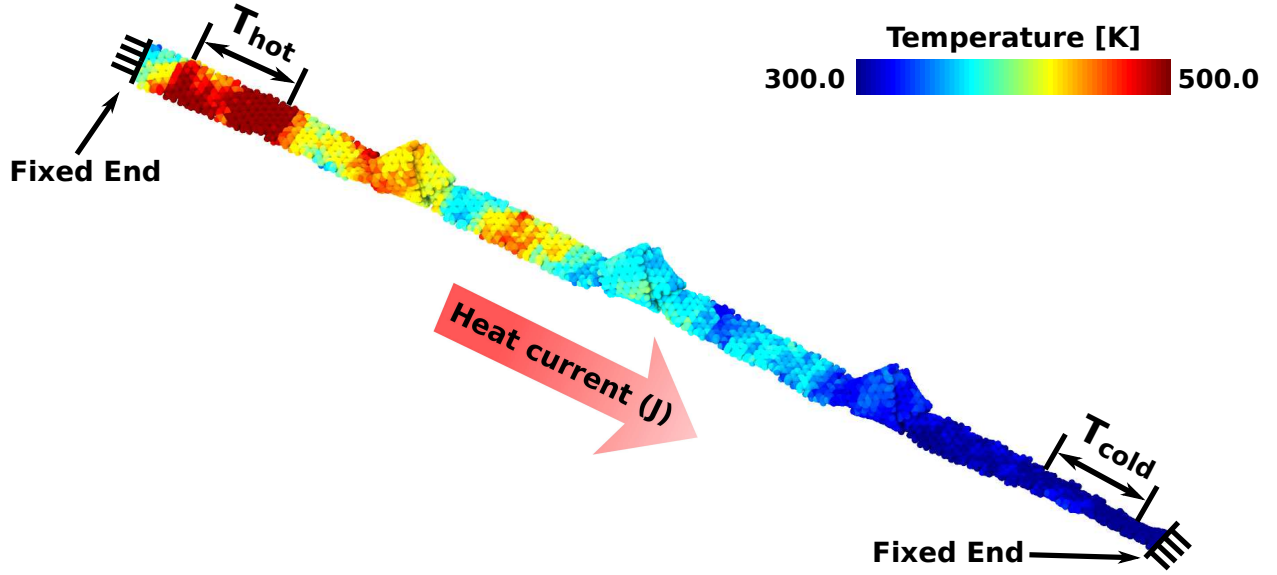


Figure 2: Scheme of the simulation setup of generating a temperature gradient in a knotted GNR. Both GNR ends are fixed and the heat baths are indicated for the hot and cold reservoir. Atoms are colored accordingly to their spatially-averaged atomic temperature t , where the average considers for all atoms within a cutoff distance of 10 Å to the central atom. The temperature color bar scale is shown at the upper right.

of the thermal gradient is different from that of the flat regions without knots. Thus, the knots behave as boundary resistances in which the effective thermal conductivity is reduced due to additional phonon scattering at the knot regions.

In order to calculate κ (the thermal conductivity of the system), we need to determine the heat flux q produced by NEMD simulations. This can be done by the time evolution of the cumulative energy in both hot and cold reservoirs, where the heat current J is obtained by the average slope from their linear fitting as shown in Figure 4 (a) for the one-knot example. In this case, $J = (0.748 + |-0.749|)/2$. Fourier's law should only be applied to regions where there is a linear relationship between temperature and position. The thermal conductivity of a region is calculated by just dividing the heat flux by the slope of fitted regions. As previously shown in Figure 3, the knots behave as materials with different conductivities κ^k . The effective thermal conductivity of the whole quasi-1D structures is calculated following the theory of heat transfer in layered composites [45, 48], where

$$\frac{1}{\kappa_{\text{eff}}} = \sum_{i=1}^{N_k+1} \frac{\phi_i}{\kappa_i} + \sum_{i=1}^{N_k} \frac{\phi_i^k}{\kappa_i^k}, \quad (3)$$

where N_k is the number of knots, $\phi_i = l_i/L_x$ and $\phi_i^k = l_i^k/L_x$ are the length fractions of flat and knotted regions, respectively. κ_i and κ_i^k are the corresponding thermal conductivities. Each κ_i is obtained by

$$\kappa_i = \frac{q}{|dT/dx|_i}, \quad (4)$$

with q being the heat flux in the whole nanoribbon and $|dT/dx|_i$ the slope of the thermal gradient of the region i . A similar expression holds with knotted regions. The Equation 3 has already been applied to nanomaterials with geometrical distortions with similar temperature profiles, as those shown in Figure 3. The dependence with the number of knots of both thermal current J and effective thermal conductivity κ_{eff} are displayed in Figure 4 (b). As each knot introduces an additional thermal resistance in the structure, we observe the expected decay of both J and κ_{eff} as N_k increases.

With the heat flux obtained for all cases, we are able to calculate the Kapitza resistance that are induced by the presence of knots in the GNRs. In Table 1 we show the temperature jumps ΔT that appear in each knot for nanoribbons with one, two and three knots. As the number of knots increases, ΔT decreases but these discontinuities in the temperature

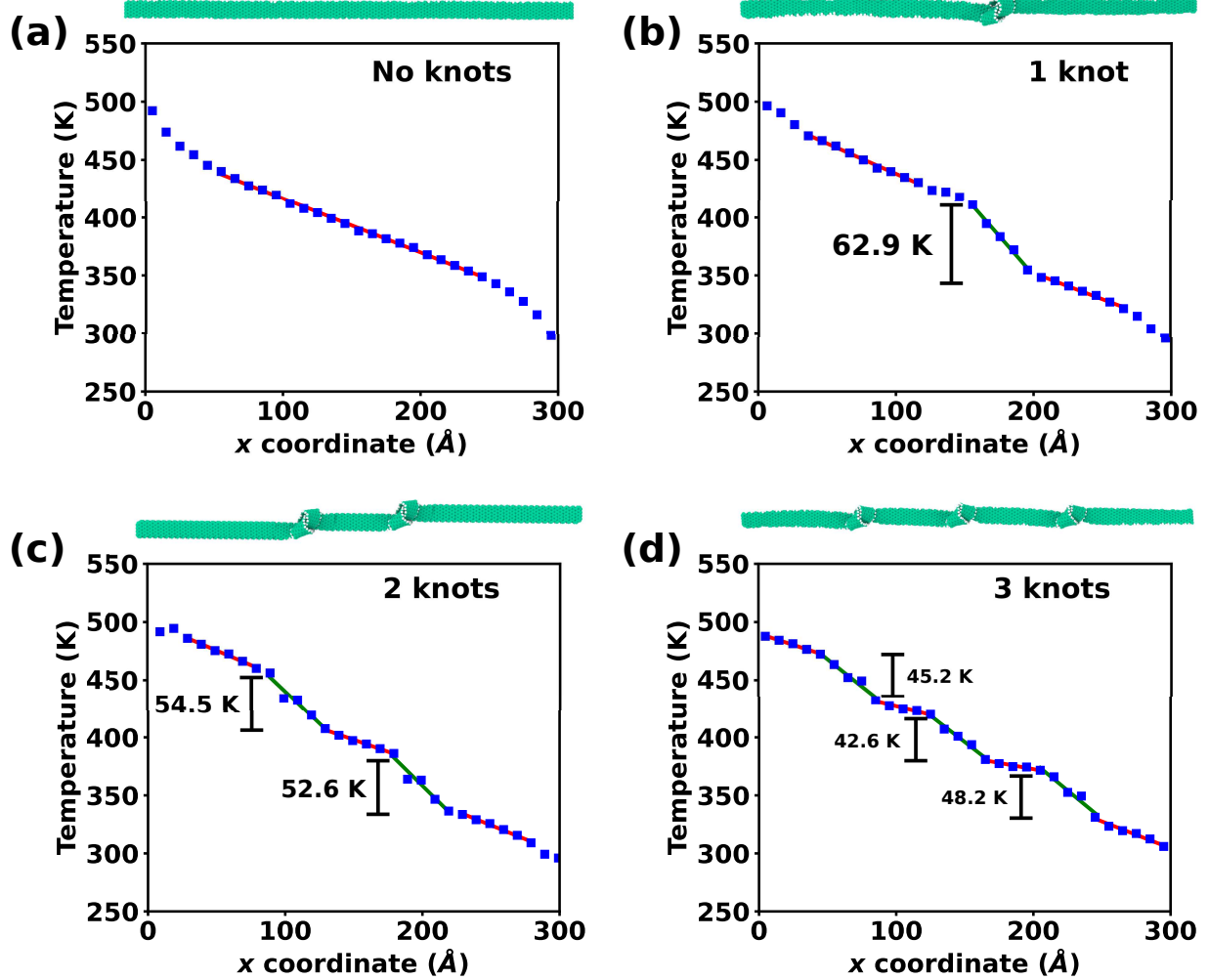


Figure 3: Temperature profiles of the cases with (a) zero, (b) one, (c) two, and (d) three knots. Red lines correspond to linear regression lines in regions where there are no knots and a linear behavior between temperature and position (where the Fourier’s law still holds). Green lines are the corresponding fittings inside regions where the knots are located. Above each profile, a schematic of the system is displayed to make clearer the effect of each knot. Also, the temperature jumps ΔT caused by the knots are also highlighted.

profiles have similar values within a given structure. The corresponding values of the resistance R introduced by each knot are almost the same. As the number of knots increases, the heat decreases in the same way to keep the ratio $\Delta T/q$ close to a constant value. Although R values for each individual knot are approximately the same, the overall thermal resistance of nanoribbons with two and three knots are, respectively, two and three times higher than that of GNRs with a single knot. This occurs because the resistance of each knot sums up as they are associated in series.

Lastly, we considered a knotted GNR where one of the knots is displaced relative to the others in order to investigate the thermal transport in asymmetrically placed knots in nanoribbons. This was motivated by previous works [36, 37, 49, 50, 51, 52] that thermal rectification appears in asymmetrical graphene and MoS₂ nanoribbons. In other words, the presence of asymmetry indicates that when the hot and cold reservoirs are reversed, the induced heat flux should be different. Figure 5 (a) shows the asymmetrical knotted GNR studied here, where the first two knots are 100 Å apart and the last knot is 50 Å distant from the second one. Two regions near the fixed ends of the structure are thermostatted at temperatures T_{left} and T_{right} . The heat flux vector points in the forward (backward) direction when $T_{\text{left}} > T_{\text{right}}$ ($T_{\text{left}} < T_{\text{right}}$). Figure 5 (b) shows the temperature profiles of both forward and backward cases. The profile of the backward case is essentially a mirror inversion of the forward case, showing that they are likely to present the same conductivity. The accumulated energy for GNRs with three knots is shown in Figure 5 (c). We compared cases with

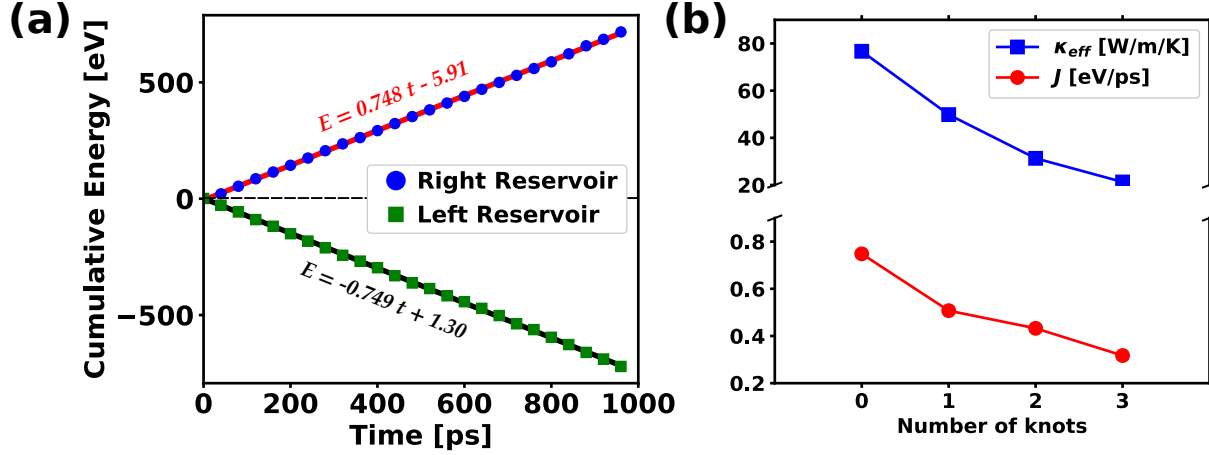


Figure 4: Calculation of the heat current. (a) Time evolution of the cumulative energy added/subtracted in the heat baths and their corresponding linear fittings showing the coefficients where the slope allows to estimate the heat current J in each reservoir. The total J is the arithmetic average of the values for each individual reservoir. (b) The behavior of the obtained heat current effective thermal conductivity κ_{eff} calculated from Equation 3.

Table 1: Temperature jumps ΔT and their corresponding interfacial (Kapitza) thermal resistances R induced by each knot for GNRs with one, two, and three knots.

Number of knots	ΔT [K]	$R \times 10^{-10}$ [m ² /W·K]
1	62.9	2.59
2	54.5	2.63
	52.6	2.54
3	45.2	2.98
	42.5	2.81
	48.2	3.18

a symmetrical arrangement of the three knots and the asymmetrical cases (forward and backward), and we observed that the cumulative energy at both heat reservoirs for all cases possess almost the same value after running for 1 ns, in which this difference ($\sim 0.7\%$) is close to the error to reach the steady state ($\sim 0.5\%$). To quantify the thermal rectification, we computed the rectification factor

$$\eta = \frac{q_f}{q_b} - 1, \quad (5)$$

where q_f (q_b) is the heat flux in the forward (backward) direction. For our case of asymmetrically arranged knots, we obtain $\eta \sim 0.3\%$. For comparison, rectification factors computed with NEMD for asymmetrical GNRs and MoS₂ range from 1 – 25% [36, 37, 50], showing that for the cases considered here, the rectification in knotted GNRs does not reach values large enough to consider them as thermal diodes.

4 Conclusions

We studied the effect of structural knots in the thermal transport of graphene nanoribbons using non-equilibrium molecular dynamics simulations. The influence of the number of knots on the heat current was investigated by considering cases where one, two, and three knots. We observed that there is a temperature jump at the position of each knot,

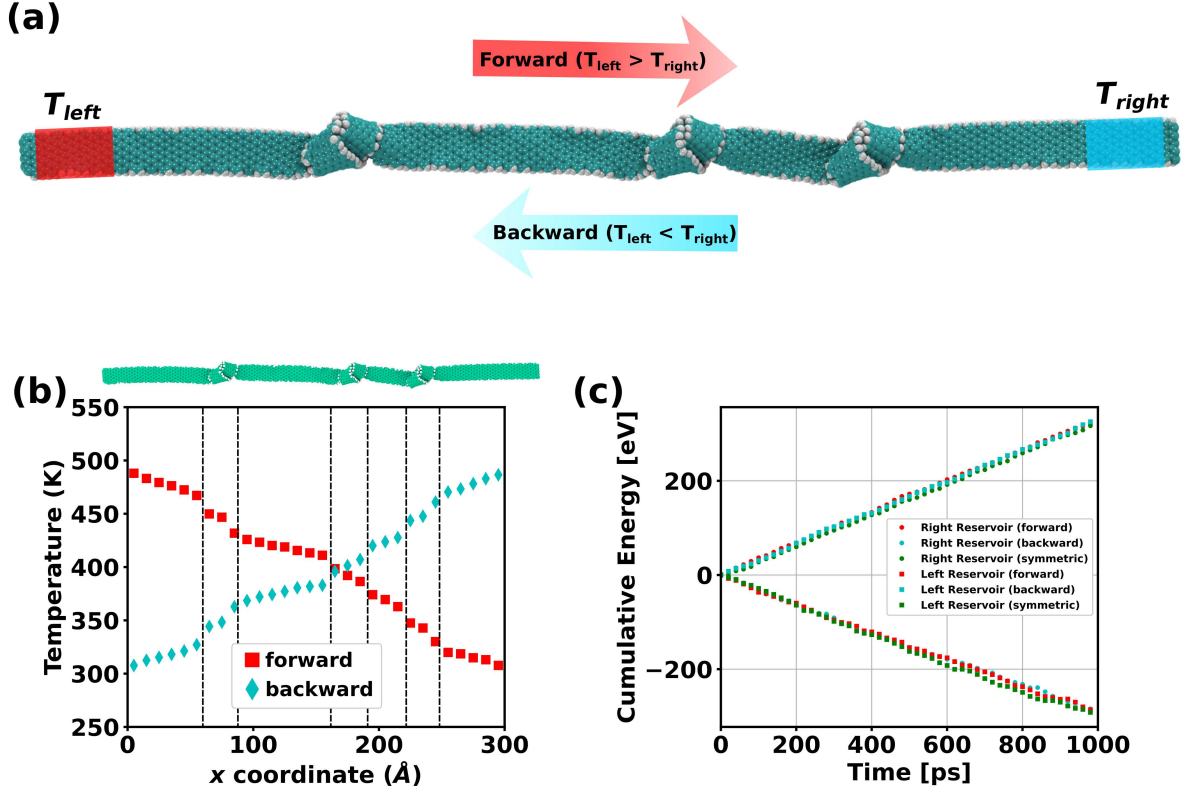


Figure 5: Thermal rectification in asymmetrically-placed three-knot GNRs. (a) Simulation setup, where the distance between each successive knot is different. (b) Temperature profile corresponding to the forward (red squares) and backward (cyan diamonds). (c) Time evolution of the cumulative energy subtracted (added) to the hot (cold) reservoirs.

which is an effect similar to interfacial Kapitza resistance present between two different materials and/or single materials with defects and/or lattice distortions. Our study also demonstrates that in the three-knot nanoribbon case, the heat current is insensitive to the relative position of the middle knot and the direction of the energy flux through the system. Thus, for the cases considered here, the effect of thermal rectification is not significant.

Acknowledgments

This work was financed by Sao Paulo State Research Support Foundation (FAPESP). We also thank the Center for Computing in Engineering and Sciences at Unicamp for financial support through the FAPESP/CEPID Grants #2013/08293-7 and #2018/11352-7.

References

- [1] Katsunori Wakabayashi, Ken-Ichi Sasaki, Takeshi Nakanishi, and Toshiaki Enoki. Electronic states of graphene nanoribbons and analytical solutions. *Science and technology of advanced materials*, 11(5):054504, oct 2010.
- [2] Young-Woo Son, Marvin L Cohen, and Steven G Louie. Energy gaps in graphene nanoribbons. *Physical Review Letters*, 97(21):216803, nov 2006.
- [3] K Nakada, M Fujita, G Dresselhaus, and MS Dresselhaus. Edge state in graphene ribbons: Nanometer size effect and edge shape dependence. *Physical review. B, Condensed matter*, 54(24):17954–17961, dec 1996.
- [4] J Jiang, W Lu, and J Bernholc. Edge states and optical transition energies in carbon nanoribbons. *Physical Review Letters*, 101(24):246803, dec 2008.

- [5] Fangzhou Zhao, Ting Cao, and Steven G Louie. Topological phases in graphene nanoribbons tuned by electric fields. *Physical Review Letters*, 127(16):166401, oct 2021.
- [6] Haomin Wang, Hui Shan Wang, Chuanxu Ma, Lingxiu Chen, Chengxin Jiang, Chen Chen, Xiaoming Xie, An-Ping Li, and Xinran Wang. Graphene nanoribbons for quantum electronics. *Nature Reviews Physics*, 3(12):791–802, dec 2021.
- [7] Z. Aksamija and I. Knezevic. Thermal transport in graphene nanoribbons supported on SiO. *Physical Review B*, 86(16):165426, oct 2012.
- [8] Giorgia Fugallo and Luciano Colombo. Calculating lattice thermal conductivity: a synopsis. *Physica Scripta*, 93(4):043002, apr 2018.
- [9] Yan Wang, Bo Qiu, and Xiulin Ruan. Edge effect on thermal transport in graphene nanoribbons: A phonon localization mechanism beyond edge roughness scattering. *Applied physics letters*, 101(1):013101, jul 2012.
- [10] Jinming Cai, Pascal Ruffieux, Rached Jaafar, Marco Bieri, Thomas Braun, Stephan Blankenburg, Matthias Muoth, Ari P Seitsonen, Moussa Saleh, Xinliang Feng, Klaus Müllen, and Roman Fasel. Atomically precise bottom-up fabrication of graphene nanoribbons. *Nature*, 466(7305):470–473, jul 2010.
- [11] Xiaolin Li, Xinran Wang, Li Zhang, Sangwon Lee, and Hongjie Dai. Chemically derived, ultrasoft graphene nanoribbon semiconductors. *Science*, 319(5867):1229–1232, feb 2008.
- [12] Liying Jiao, Li Zhang, Xinran Wang, Georgi Diankov, and Hongjie Dai. Narrow graphene nanoribbons from carbon nanotubes. *Nature*, 458(7240):877–880, apr 2009.
- [13] Xinran Wang, Yijian Ouyang, Xiaolin Li, Hailiang Wang, Jing Guo, and Hongjie Dai. Room-temperature all-semiconducting sub-10-nm graphene nanoribbon field-effect transistors. *Physical Review Letters*, 100(20):206803, may 2008.
- [14] Junjie Chen and Baofang Liu. Ballistic heat conduction characteristics of graphene nanoribbons. *Physica E: Low-dimensional Systems and Nanostructures*, 139:115146, may 2022.
- [15] Bikash Mandal, Sunandan Sarkar, Anup Pramanik, and Pranab Sarkar. Doped defective graphene nanoribbons: a new class of materials with novel spin filtering properties. *RSC Adv.*, 4(91):49946–49952, sep 2014.
- [16] Lin Du, Tam N. Nguyen, Ari Gilman, André R. Muniz, and Dimitrios Maroudas. Tuning the band structure of graphene nanoribbons through defect-interaction-driven edge patterning. *Physical Review B*, 96(24):245422, dec 2017.
- [17] I Nikiforov, B Hourahine, Th Frauenheim, and T Dumitrică. Formation of helices in graphene nanoribbons under torsion. *The Journal of Physical Chemistry Letters*, 5(23):4083–4087, dec 2014.
- [18] Alexandre F. Fonseca. Twisting or untwisting graphene twisted nanoribbons without rotation. *Physical Review B*, 104(4):045401, jul 2021.
- [19] Rajesh Thakur, P.K. Ahluwalia, Ashok Kumar, Brij Mohan, and Raman Sharma. Electronic structure and carrier mobilities of twisted graphene helix. *Physica E: Low-dimensional Systems and Nanostructures*, 124:114280, oct 2020.
- [20] Alireza Shahabi, Hailong Wang, and Moneesh Upmanyu. Shaping van der waals nanoribbons via torsional constraints: scrolls, folds and supercoils. *Scientific Reports*, 4:7004, nov 2014.
- [21] M. Saiz-Bretín, F. Domínguez-Adame, and A.V. Malyshev. Twisted graphene nanoribbons as nonlinear nano-electronic devices. *Carbon*, 149:587–593, aug 2019.
- [22] Te-Hua Fang, Win-Jin Chang, Yu-Lun Feng, and Deng-Maw Lu. Torsional characteristics of graphene nanoribbons encapsulated in single-walled carbon nanotubes. *Physica E: Low-dimensional Systems and Nanostructures*, 83:263–267, sep 2016.
- [23] O. O. Kit, T. Tallinen, L. Mahadevan, J. Timonen, and P. Koskinen. Twisting graphene nanoribbons into carbon nanotubes. *Physical Review B*, 85(8):085428, feb 2012.
- [24] Kyle Rego and Vincent Meunier. Carbon nanotube knots. *AIP advances*, 9(2):025030, feb 2019.
- [25] Federico Bosia, Emiliano Lepore, Noe T. Alvarez, Peter Miller, Vesselin Shanov, and Nicola M. Pugno. Knotted synthetic polymer or carbon nanotube microfibrils with enhanced toughness, up to 1400 J/g. *Carbon*, 102:116–125, jun 2016.
- [26] Nicola M Pugno. The "egg of columbus" for making the world's toughest fibres. *Plos One*, 9(4):e93079, apr 2014.

- [27] Changsheng Xiang, Colin C Young, Xuan Wang, Zheng Yan, Chi-Chau Hwang, Gabriel Cerioti, Jian Lin, Junichiro Kono, Matteo Pasquali, and James M Tour. Large flake graphene oxide fibers with unconventional 100% knot efficiency and highly aligned small flake graphene oxide fibers. *Advanced Materials*, 25(33):4592–4597, sep 2013.
- [28] Maria F Pantano, Alice Berardo, and Nicola M Pugno. Tightening slip knots in raw and degummed silk to increase toughness without losing strength. *Scientific Reports*, 6:18222, feb 2016.
- [29] R. Kagimura, M. S. C. Mazzoni, and H. Chacham. Knots in a graphene nanoribbon. *Physical Review B*, 85(12):125415, mar 2012.
- [30] Steve Plimpton. Fast parallel algorithms for short-range molecular dynamics. *Journal of Computational Physics*, 117(1):1–19, mar 1995.
- [31] L. Lindsay and D. A. Broido. Optimized tersoff and brenner empirical potential parameters for lattice dynamics and phonon thermal transport in carbon nanotubes and graphene. *Physical Review B*, 81(20):205441, may 2010.
- [32] Xiangfan Xu, Luiz F C Pereira, Yu Wang, Jing Wu, Kaiwen Zhang, Xiangming Zhao, Sukang Bae, Cong Tinh Bui, Rongguo Xie, John T L Thong, Byung Hee Hong, Kian Ping Loh, Davide Donadio, Baowen Li, and Barbaros Özyilmaz. Length-dependent thermal conductivity in suspended single-layer graphene. *Nature Communications*, 5:3689, apr 2014.
- [33] Zheyong Fan, Luiz Felipe C. Pereira, Petri Hirvonen, Mikko M. Ervasti, Ken R. Elder, Davide Donadio, Tapio Ala-Nissila, and Ari Harju. Thermal conductivity decomposition in two-dimensional materials: Application to graphene. *Physical Review B*, 95(14):144309, apr 2017.
- [34] Alexander Stukowski. Visualization and analysis of atomistic simulation data with OVITO—the open visualization tool. *Modelling and Simulation in Materials Science and Engineering*, 18(1):015012, jan 2010.
- [35] GERALD L. Pollack. Kapitza resistance. *Reviews of Modern Physics*, 41(1):48–81, jan 1969.
- [36] Yan Wang, Ajit Vallabhaneni, Jiuning Hu, Bo Qiu, Yong P Chen, and Xiulin Ruan. Phonon lateral confinement enables thermal rectification in asymmetric single-material nanostructures. *Nano Letters*, 14(2):592–596, feb 2014.
- [37] Leonardo Medrano Sandomas, Rafael Gutierrez, Arezoo Dianat, and Giovanni Cuniberti. Engineering thermal rectification in MoS₂ nanoribbons: a non-equilibrium molecular dynamics study. *RSC Adv.*, 5(67):54345–54351, 2015.
- [38] Zheyong Fan, Petri Hirvonen, Luiz Felipe C Pereira, Mikko M Ervasti, Ken R Elder, Davide Donadio, Ari Harju, and Tapio Ala-Nissila. Bimodal grain-size scaling of thermal transport in polycrystalline graphene from large-scale molecular dynamics simulations. *Nano Letters*, 17(10):5919–5924, oct 2017.
- [39] Yang Kang, Fuyan Duan, Shaoxin Shangguan, Yixin Zhang, Tianpei Zhou, and Bingcheng Si. Thermal transport of graphene sheets with fractal defects. *Molecules (Basel, Switzerland)*, 23(12), dec 2018.
- [40] Alexey N. Volkov, Takuma Shiga, David Nicholson, Junichiro Shiomi, and Leonid V. Zhigilei. Effect of bending buckling of carbon nanotubes on thermal conductivity of carbon nanotube materials. *Journal of applied physics*, 111(5):053501, mar 2012.
- [41] Zhengxing Huang, Zhen’an Tang, Jun Yu, and Suyuan Bai. Temperature-dependent thermal conductivity of bent carbon nanotubes by molecular dynamics simulation. *Journal of applied physics*, 109(10):104316, may 2011.
- [42] Fumio Nishimura, Takuma Shiga, Shigeo Maruyama, Kazuyuki Watanabe, and Junichiro Shiomi. Thermal conductance of buckled carbon nanotubes. *Japanese journal of applied physics*, 51(1):015102, jan 2012.
- [43] Victor Lee, Renkun Chen, and Chih-Wei Chang. Probing the limit of one-dimensional heat transfer under extreme bending strain. *Physical Review B*, 87(3):035406, jan 2013.
- [44] C W Chang, D Okawa, H Garcia, A Majumdar, and A Zettl. Nanotube phonon waveguide. *Physical Review Letters*, 99(4):045901, jul 2007.
- [45] Jihong Al-Ghalith and Traian Dumitrică. *Nano-scale Heat Transfer in Nanostructures: Toward Understanding and Engineering Thermal Transport*. Springer Briefs in Applied Sciences and Technology: Thermal Engineering and Applied Science. Springer International Publishing, Cham, 2018.
- [46] Philip B. Allen. Size effects in thermal conduction by phonons. *Physical Review B*, 90(5):054301, aug 2014.
- [47] Andrea Cepellotti and Nicola Marzari. Boltzmann transport in nanostructures as a friction effect. *Nano Letters*, 17(8):4675–4682, aug 2017.
- [48] Fergany Badry and Karim Ahmed. A new model for the effective thermal conductivity of polycrystalline solids. *AIP advances*, 10(10):105021, oct 2020.

-
- [49] Xavier Cartoixà, Luciano Colombo, and Riccardo Rurali. Thermal rectification by design in telescopic si nanowires. *Nano Letters*, 15(12):8255–8259, dec 2015.
 - [50] Haidong Wang, Shiqian Hu, Koji Takahashi, Xing Zhang, Hiroshi Takamatsu, and Jie Chen. Experimental study of thermal rectification in suspended monolayer graphene. *Nature Communications*, 8:15843, jun 2017.
 - [51] Xiao Yang, Xinghua Zheng, Qiushi Liu, Ting Zhang, Ye Bai, Zheng Yang, Haisheng Chen, and Ming Liu. Experimental study on thermal conductivity and rectification in suspended monolayer mos2. *ACS Applied Materials & Interfaces*, 12(25):28306–28312, jun 2020.
 - [52] Fayong Liu, Manoharan Muruganathan, Yu Feng, Shinichi Ogawa, Yukinori Morita, Chunmeng Liu, Jiayu Guo, Marek Schmidt, and Hiroshi Mizuta. Thermal rectification on asymmetric suspended graphene nanomesh devices. *Nano Futures*, 5(4):045002, dec 2021.